

# 1 **1. Supplemental Materials and methods**

## 2 **1.1 Reagents and chemicals**

3 DMEM and bovine calf serum were purchased from Gibco Co. (Carlsbad, CA,  
4 USA). Ang II (HY-13948) was obtained from MCE (USA). Antibodies against  
5 PGAM2 (SAB2702034) were obtained from Sigma-Aldrich (St Louis, MO, USA).  
6 Antibodies against phospho-mTOR (5536S), phospho-4EBP1 (2855S), and phospho-  
7 p65 (3033S) were obtained from Cell Signaling Technology (Danvers, MA, USA).  
8 Antibodies against HSP90 (13171-1-AP), mTOR (66888-1-Ig), 4EBP1 (60246-1-Ig),  
9 GAPDH (60004-1-Ig) and  $\beta$ -actin (66009-1-Ig) were obtained from Proteintech  
10 (Wuhan, China). Ganetespib (S1159) was obtained from Selleck (USA). PLA kits  
11 were obtained from Sigma-Aldrich (St Louis, MO, USA).

## 12 **1.2 Ethics statement**

13 In the present study, male Wistar rats weighing  $200 \pm 10$  g and 1- to 3-day-old  
14 Wistar rats were used in the current studies. The adult rats were maintained under a  
15 12-hour light/dark cycle in pathogen-free conditions, with unrestricted access to  
16 standard rat chow and tap water. All experimental procedures were in accordance  
17 with the guidelines from Directive 2010/63/EU of the European Parliament on the  
18 protection of animals used for scientific purposes and the NIH Guide for the Care and  
19 Use of Laboratory Animals and approved by the Animal Care and Use Committee of  
20 Jinan Central Hospital (JNCHIAUCUC202242).

## 21 **1.3 Primary culture of neonatal rat ventricular myocytes (NRVMs)**

22 Wistar rats aged 1 to 3 days were anesthetized by inhaling 2% isoflurane for 3  
23 minutes. The ventricles were subsequently minced and digested in phosphate-buffered  
24 saline (PBS) supplemented with 200 U of type II collagenase and 0.4% horse serum,  
25 undergoing three digestion cycles. Following digestion, the cells were centrifuged and  
26 resuspended in Dulbecco's modified Eagle's medium (DMEM) containing 5% fetal  
27 bovine serum and 8% horse serum. To remove non-cardiomyocytes, a single  
28 preplating step of 1.5 hours was conducted, allowing non-cardiomyocytes to adhere to  
29 the bottom of the culture dishes while the unattached myocytes remained in  
30 suspension. The unattached myocytes were then plated at a density of  $1 \times 10^5$  cells/ml  
31 in the same medium supplemented with 0.1 mM 5-Bromo-2-deoxyUridine (BrdU).  
32 The identity of the NRVMs was confirmed through morphological assessment and  
33 immunostaining with an  $\alpha$ -actin antibody, revealing that over 95% of the cells were  
34 indeed identified as NRVMs.

#### 35 **1.4 Experimental Animals**

36 For lentiviral vector-mediated gene transfer in rat, wild-type male Wistar rats  
37 were treated with adeno-associated virus serotype 9 (AAV9) carrying the PGAM2  
38 shRNA knockdown vector, HSP90 overexpression vectors or a negative control virus  
39 delivered through the jugular vein two weeks prior to infusion with Ang II. Male  
40 Wistar rats were lightly anaesthetized using 3% isoflurane inhalation. Ang II infusion  
41 was conducted using subcutaneously implanted osmotic mini-pumps (200 ng/kg/min)  
42 for a duration of four weeks. The rats were randomly divided into different groups

43 based on their treatment with or without Ang II. The control group received sterile  
44 saline pumps, with six rats in each group.

### 45 **1.5 Echocardiography of rat**

46 The rats were lightly anesthetized using 3% isoflurane inhalation. Imaging was  
47 performed with the animals positioned in the left lateral decubitus position, utilizing a  
48 VisualSonics Vevo 3100LT machine. Images were acquired using M-mode,  
49 two-dimensional (2-D), and pulse wave (PW) Doppler techniques. All measurements  
50 were calculated by the same observer based on the average of six consecutive cardiac  
51 cycles.

### 52 **1.6 Cardiovascular Magnetic Resonance scans**

53 The rats underwent scanning using 9.4 T small animal magnetic resonance  
54 imaging (MRI) (Bruker, BioSpec94/20USR, USA). Briefly, each rat was anesthetized  
55 with 3% isoflurane and positioned in a prone orientation within the radiofrequency  
56 coil. The chest of each rat was centered in the coil, electrodes were inserted into the  
57 forelimb and right hindlimb, and a respiration sensor was affixed to the abdomen.  
58 MRI scans were conducted once the respiration and electrocardiogram (ECG) signals  
59 stabilized. A three-plane localization sequence scan was performed on the chest,  
60 followed by the acquisition of four-chamber, two-chamber, and short-axis images of  
61 the heart based on the localization image. The parameters were as follows: echo time  
62 (TE) of 2 ms, repetition time (TR) of 8.00 ms, flip angle (FA) of 15°, slice thickness  
63 of 1.5 mm, field of view (FOV) of 40 mm × 40 mm, with a matrix size of 192×192.

64 The number of excitations (NEX) was set to four, and 15 film images were collected  
65 per cardiac cycle. The total scan duration was 30 to 40 minutes. Global cardiac  
66 function was assessed by analyzing the cine images using cvi42 software (Circle,  
67 Calgary, Alberta, Canada).

### 68 **1.7 Hematoxylin and eosin (H&E) staining**

69 Myocardial tissues were sectioned in a cross-sectional orientation, fixed in a 4%  
70 paraformaldehyde solution, and subsequently embedded in paraffin for tissue  
71 sectioning. Hematoxylin and eosin (H&E) staining was performed on the tissue  
72 sections. Images were captured using a bright field microscope (Olympus BX53) and  
73 analyzed for cell size using Image Pro Plus 7.0 software. The data presented represent  
74 analyses from six independent experiments.

### 75 **1.8 Immunofluorescence staining**

76 For immunofluorescence staining, cells from each experimental group were  
77 cultured on coverslips and subjected to various treatments as indicated. Subsequently,  
78 the cells were fixed in 4% paraformaldehyde for 15 min at room temperature, and  
79 permeabilized with 0.3% Triton/PBS for three min. After blocking with 10% donkey  
80 serum for 45 min, cells were incubated overnight at 4 °C with rabbit anti-PGAM2  
81 antibody (dilution 1:200). Then, cells in each group were incubated with Alexa Fluor  
82 488 conjugated donkey Anti-Rabbit IgG secondary antibody for one hour. Finally, the  
83 cells were incubated with DAPI-containing mounting media and observed using a

84 fluorescence microscope (Olympus, Japan). The immunofluorescence images were  
85 quantified using Image J software.

## 86 **1.9 Analysis of mRNA expression by real-time PCR**

87 Total RNA was extracted using TRIzol reagent (Invitrogen) in accordance with  
88 the manufacturer's instructions. cDNA synthesis was conducted using the PrimeScript  
89 RT reagent kit with gDNA Eraser (Takara), utilizing 1  $\mu$ g of RNA. Real-time PCR  
90 amplification reactions were performed in triplicate with the SYBR Premix Ex Taq kit  
91 containing ROX (Takara) on an ABI Prism 7900 Real-Time PCR machine. The  
92 expression levels of the gene of interest were quantified using the  $\Delta\Delta$ CT method and  
93 normalized against  $\beta$ -actin mRNA levels. The results are presented as fold changes in  
94 gene expression relative to the control groups. The primer sequences used for PCR  
95 amplification were as follows: PGAM2 forward,  
96 5'-GTCCTTATTGCAGCCCATGG-3' and reverse,  
97 5'-ACCCACTCTCACTTTGCCTT-3'; atrial natriuretic peptide (ANP) forward,  
98 5'-GGGGGTAGGATTGACAGGAT-3 and reverse,  
99 5'-GGATCTTTTGCATCTGCTC-3; and brain natriuretic peptide (BNP) forward, 5-  
100 GCTGCTTTGGGCAGAAGATA -3' and reverse, 5-  
101 GGAGTCTGCAGCCAGGAGGT -3;  $\beta$ -myosin heavy chain ( $\beta$ -MHC) forward, 5'-  
102 CGCTCAGTCATGGCGGAT-3' and reverse, 5'-GCCCAAATGCAGCCAT- 3';  
103 Hsp90 forward, 5'-CCAAGGACCAGGTTGCTAACTCA-3' and reverse, 5'-  
104 GACACCAAGGTCTTGCCCTCA- 3';  $\beta$ -actin forward, 5-  
105 CGTTGACATCCGTAAAGACC -3 and reverse, 5-

106 TAGAGCCACCAATCCACACA -3. All real-time experiments have been repeated  
107 three times to ensure reproducibility and accuracy of the results.

### 108 **1.10 RNA interference (RNAi)**

109 NRVMs were transfected with siRNA targeting PGAM2 or HSP90, or with  
110 scrambled siRNA at a concentration of 50 nM for 24 h using lipofectamine 2000,  
111 following the manufacturer's protocol (Invitrogen, USA). The efficiency of RNAi was  
112 determined by Western blotting or qPCR analysis.

### 113 **1.11 Co-Immunoprecipitation (Co-IP)**

114 After various treatments, cells were lysed in ice-cold immunoprecipitation  
115 lysis/wash buffer (100  $\mu$ L/ $1 \times 10^6$  cells, Servicebio) at 4 °C for 30 min, followed by  
116 centrifugation at 12,000 rpm for 10 minutes. An equal amount of cell lysates (200  $\mu$ L)  
117 was incubated overnight at 4 °C with anti-flag, anti-HSP90, or IgG antibody, along  
118 with A/G agarose (Beyotime, 20  $\mu$ L). Following incubation, the samples were  
119 centrifuged at 1000 g for 10 minutes, and the supernatant was discarded. The  
120 immunoprecipitated complexes were washed three times with lysis buffer, and then  
121 eluted in sample buffer containing 1 $\times$ sodium dodecyl sulfate (SDS) loading buffer by  
122 boiling for SDS-PAGE. Subsequently, the complexes were subjected to immunoblot  
123 analysis to detect the interacting proteins.

### 124 **1.12 LC-MS/MS Analysis**

125 After transfected with flag-PGAM2 and flag-Ctr vectors, NRVMs were lysed  
126 in ice-cold immunoprecipitation lysis/wash buffer. Flag antibody was added to the

127 samples for IP experiment. Then, the LC-MS/MS analysis was carried out by PTM  
128 Bio Co., Ltd (Zhejiang, China). Finally, we screened out the proteins that could bind  
129 to PGAM2 according to the score and the mass of detected proteins.

### 130 **1.13 Western blot analysis**

131 Cells were lysed in a protein lysis buffer containing 1% SDS, 25 mM Tris-HCl  
132 (pH 7.5), 100 mM NaCl, 4 mM EDTA, 1 mM PMSF, 10 mg/mL leupeptin, and 10  
133 mg/mL soybean trypsin inhibitor. The protein concentration of the lysates was  
134 determined using the Coomassie Brilliant Blue protein assay. Subsequently, protein  
135 extracts from NRVMs (10 µg) were loaded onto 12% or 6% SDS polyacrylamide gels  
136 for electrophoresis and then transferred to a PVDF membrane. Following the transfer,  
137 the membranes were incubated with the appropriate primary antibodies to detect the  
138 proteins of interest. The target proteins were detected with a horseradish  
139 peroxidase-conjugated IgG secondary antibody. Band intensity was quantified using  
140 ImageJ software (Bio-Rad, USA) and normalized to internal control levels.

### 141 **1.14 Proximity ligation assay (PLA)**

142 Duolink In Situ reagents from Olink Bioscience enable detection of protein  
143 interactions in tissue and cell samples prepared for microscopy. The Duolink In Situ  
144 reagents utilize in situ PLA, a proximity ligation assay technology. This assay allows  
145 for the detection of the interaction between PGAM2 and HSP90 using two primary  
146 antibodies. To visualize the interaction, a pair of oligonucleotide-labeled secondary  
147 antibodies (known as PLA probes, one PLUS and one MINUS) is utilized. These PLA

148 probes generate a signal only when they bind in proximity, with two primary  
149 antibodies that have bound to the sample in proximity. The signal from each detected  
150 pair of PLA probes is visualized as an individual fluorescent spot. These PLA signals  
151 can be quantified (counted) and assigned to a specific subcellular location based on  
152 microscopy images. All the procedures were performed according to the  
153 manufacturer's instructions.

### 154 **1.15 Homology modelling and molecular docking**

155 Homology modelling was conducted using the online program SWISS  
156 MODEL (<http://swissmodel.expasy.org/>). Initially, the primary amino acid sequence  
157 of HSP90 from the rat was uploaded to the program. The SWISS-MODEL template  
158 library (SMTL version 2020-04-08, PDB release 2020-04-03) was then searched  
159 using BLAST and HHblits to identify evolutionary related structures that match the  
160 target sequence. Based on the results obtained, a suitable template was selected for the  
161 homology modeling of the HSP90 crystal structure. The model was constructed using  
162 ProMod3, which aligns the target sequence with the chosen template. Conserved  
163 coordinates between the target and the template were copied from the template to the  
164 model, while insertions and deletions were remodeled using a fragment library. Side  
165 chains are subsequently rebuilt, and the geometry of the resulting model was  
166 optimized using a force field. If loop modeling with ProMod3 was unsuccessful, an  
167 alternative model was generated using PROMOD-II. The global and per-residue  
168 model quality was assessed using the QMEAN scoring function. The constructed  
169 model was selected for subsequent molecular docking simulation. Similar procedures



170 were employed for the homology modeling simulation of the full length PGAM2 (Rat  
171 organism) and HSP90 (Rat organism). The templates for PGAM2 and HSP90 were  
172 6H26 and 5FWM, respectively.

### 173 **1.16 Protein-protein docking simulation**

174 The online Z-DOCK server (<http://zdock.umassmed.edu/>) was utilized to  
175 perform the protein-protein docking simulations. In the simulation of HSP90 with  
176 PGAM2, the modeled HSP90 (dimer) and PGAM2 (dimer) were uploaded as Input  
177 Protein 1 and Input Protein 2 respectively. The ZDOCK 3.0.2f + IRaPPA re-ranking  
178 ZDOCK version was selected for the simulation, with no interacting residues defined.  
179 For the simulation, the top-ranking 10 predicted protein-protein interaction modes  
180 were retrieved for further evaluation.

### 181 **1.17 Statistical Analysis**

182 The data are presented as mean  $\pm$  standard deviation (SD) and were analyzed  
183 using GraphPad Prism 9.0 software (San Diego, CA, USA). To determine significant  
184 differences, a two-tailed Student's t-test was employed for comparisons between two  
185 groups, while one-way ANOVA followed by Tukey's post-hoc test was utilized for  
186 comparisons involving more than two groups. Figures were processed using Adobe  
187 Photoshop software. For samples requiring repeated measurements from a single  
188 individual, independent analyses of the data sets were conducted using two-way  
189 repeated-measures ANOVA. This analysis employed a single pooled variance and  
190 applied the Tukey correction for pairwise comparisons within groups for each data set.  
191 The exact group size (n) for each experiment is provided, and 'n' refers to biological

192 replicates rather than technical replicates. Differences with a  $p < 0.05$  were considered  
193 statistically significant.

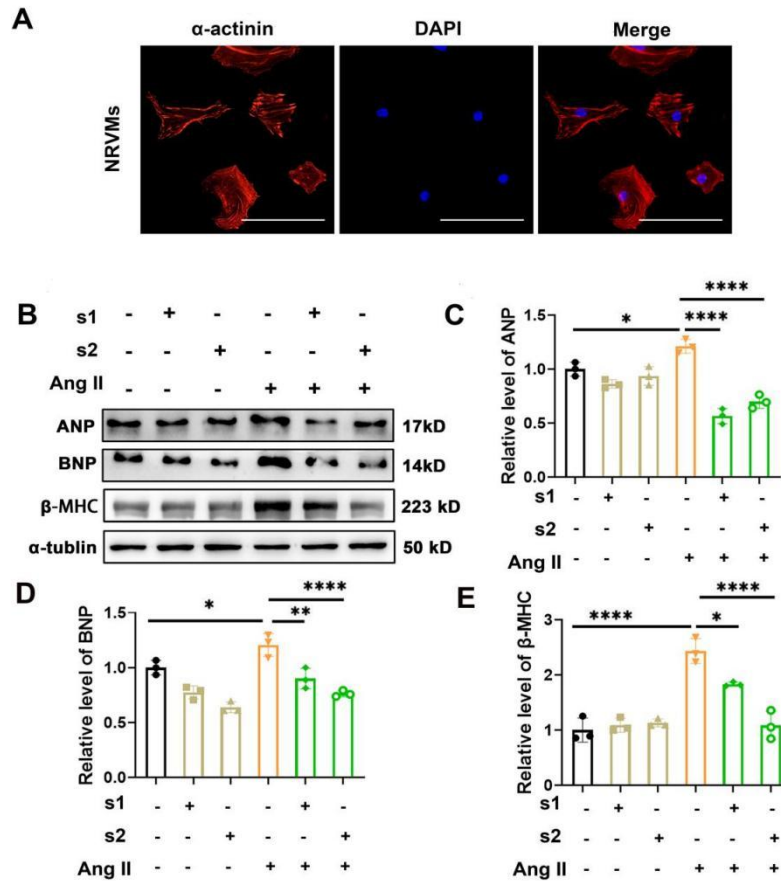
## 194 **2. Supplementary Table S1**

195 MS spectra peptide sequences and scores of HSP90 from PGAM2-IP samples.

196	<b>Sequence</b>	<b>Protein</b>	<b>Score</b>
	APFDLFENR	HSP90	95.815
197	ELHINLIPNK	HSP90	71.349
198	ELISNSSDALDK	HSP90	73.885
	ESDDKPEIEDVGSDEEEEEK	HSP90	54.834
199	HIYFITGETK	HSP90	126.24
	HLEINPDHSIIETLR	HSP90	68.944
	LGIHEDSQNR	HSP90	99.136
	NPDDITNEEYGEFYK	HSP90	185.25
	YYTSASGDEMVSLLK	HSP90	117.09

200 Single-letter abbreviations for the amino acid residues are: A, Ala; D, Asp; E, Glu; F,  
201 Phe; G, Gly; H, His; I, Ile; K, Lys; L, Leu; M, Met; N, Asn; P, Pro; Q, Gln; R, Arg;  
202 S,Ser; T, Thr; V, Val; W, Trp; Y, Tyr.

## 203 **3. Supplementary Figures**



204

205 **Supplementary Figure S1.** Identification of NRVMs and cardiac hypertrophy

206 indicators ANP, BNP and  $\beta$ -MHC expression after different treatments. (A)

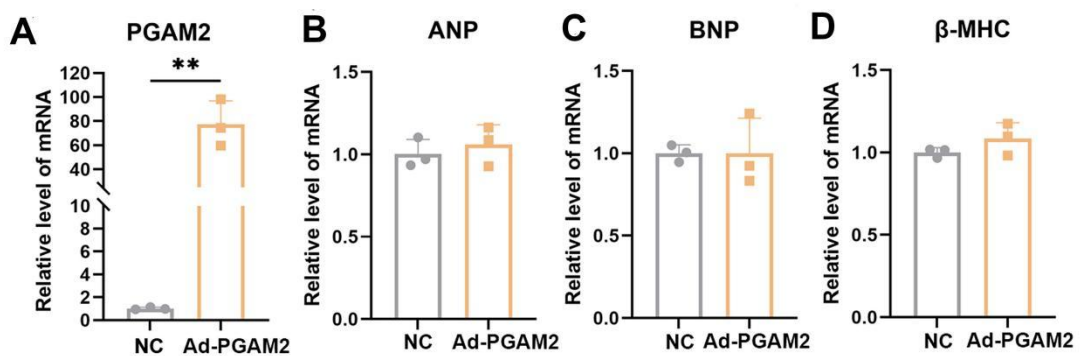
207 Immunofluorescence was performed for the identification of NRVMs. Bar = 50  $\mu$ m.

208 (B-E) Following treatment with Ang II in both the control and PGAM2 knockdown

209 groups, the protein levels of ANP, BNP and  $\beta$ -MHC were determined by western blot

210 (\*,  $P < 0.05$ . \*\*,  $P < 0.01$ . \*\*\*\*,  $P < 0.0001$ . n = 3).

211

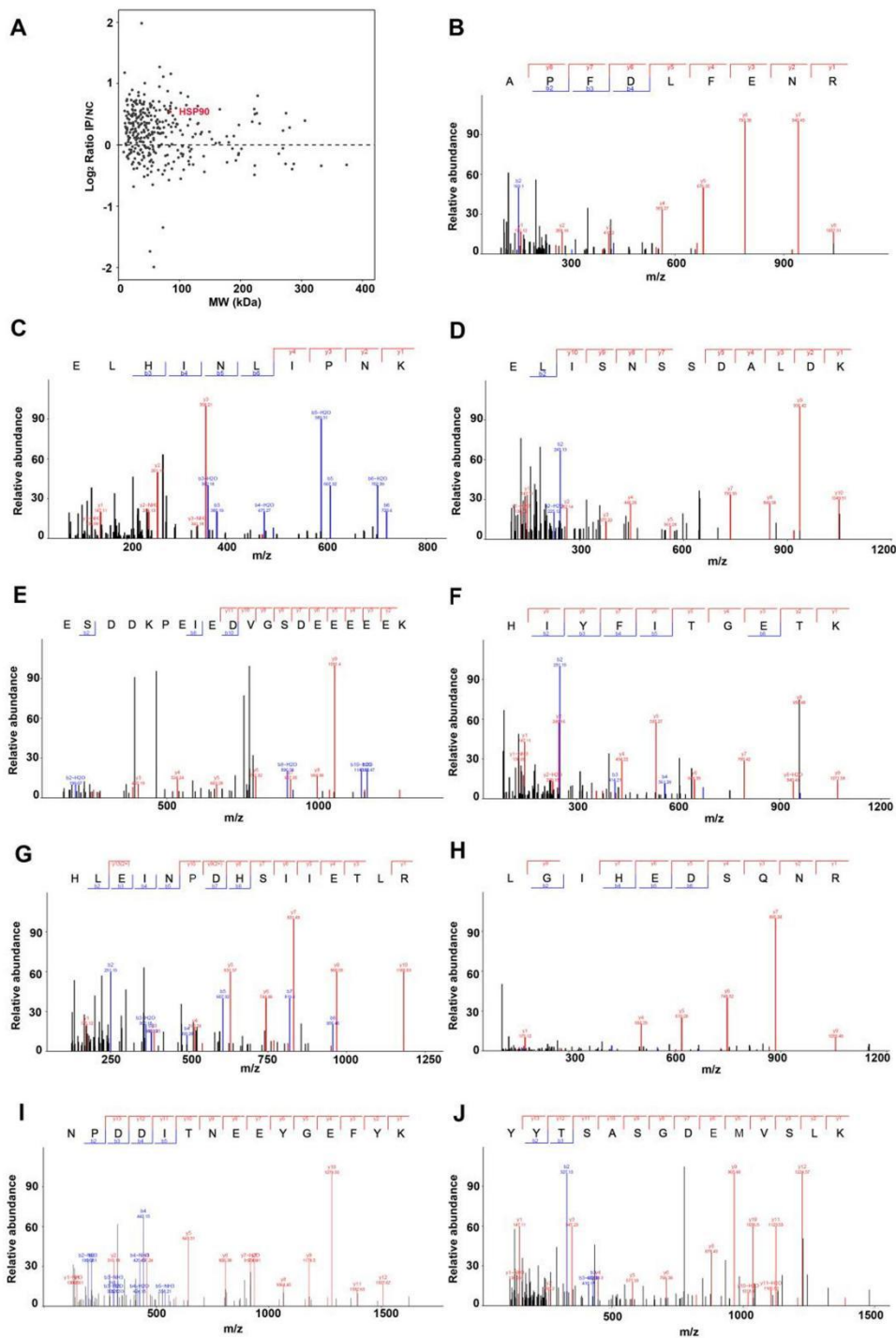


212

213 **Supplementary Figure S2.** After transfected with Ad-PGAM2 in NRVMs, the

214 relative mRNA levels of (A) PGAM2, (B) ANP, (C) BNP and (D)  $\beta$ -MHC were

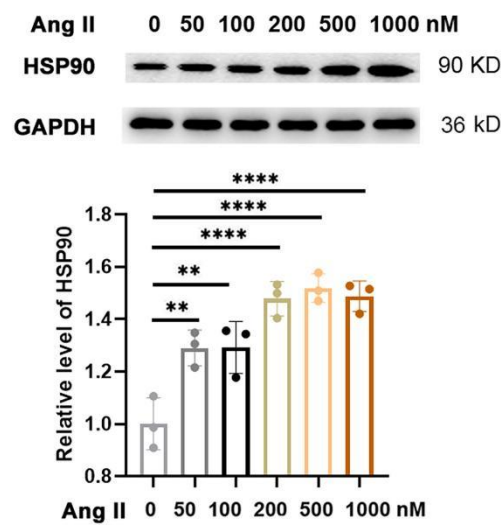
215 determined by qPCR.  $n = 3$  (\*\*,  $p < 0.01$ ).



216

217 **Supplementary Figure S3.** (A) Two-dimensional (2D) plot with log<sub>2</sub> IP/NC (log<sub>2</sub>  
 218 PGAM2-IP score/NC-IP score ratios) of the quantified proteins. The y-axis represents  
 219 the enrichment in flag-PGAM2 immunoprecipitation (PGAM2-IP) versus flag-Ctr  
 220 immunoprecipitation (NC-IP), while the x-axis represents the molecular weight (MW)  
 221 of the protein. (B-J) Mass spectrometry (MS) spectra peptides confirming the

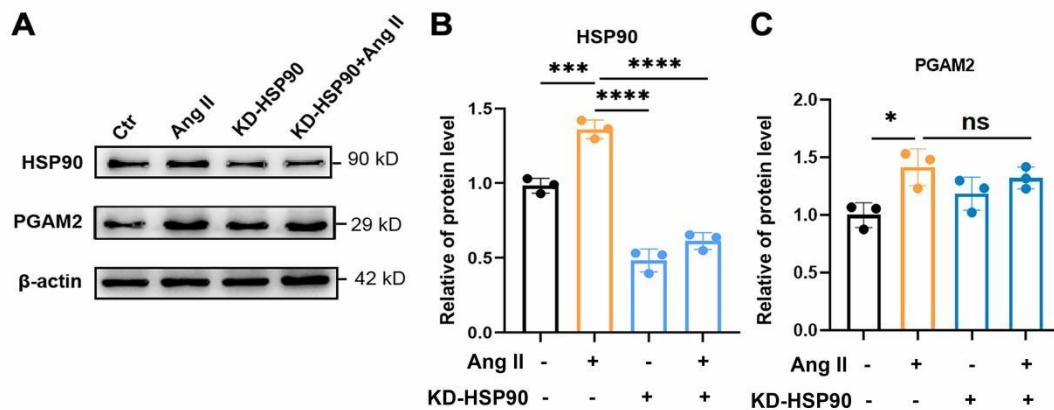
222 interaction between PGAM2 and HSP90. The identified peptides from HSP90 include  
 223 APFDLFENR (B), ELHINLIPNK (C), ELISNSSDALDK (D),  
 224 ESDDKPEIEDVGSDEEEEEK (E), HIYFITGETK (F), HLEINPDHSIIETLR (G),  
 225 LGIHEDSQNR (H), NPDDITNEEYGEFYK (I) and YYTSASGDEMVSLLK (J). The  
 226 single-letter abbreviations for the amino acid residues are as follows: A, Ala; D, Asp;  
 227 E, Glu; F, Phe; G, Gly; H, His; I, Ile; K, Lys; L, Leu; M, Met; N, Asn; P, Pro; Q, Gln;  
 228 R, Arg; S, Ser; T, Thr; V, Val; W, Trp; Y, Tyr. m/z, represents mass/charge ratio.  
 229



230

231 **Supplementary Figure S4.** Representative western blotting for HSP90 under  
 232 stimulation with different doses of Ang II and densitometric quantification (\*\*,  $P <$   
 233 0.01. \*\*\*\*,  $P < 0.0001$ .  $n = 3$ ).

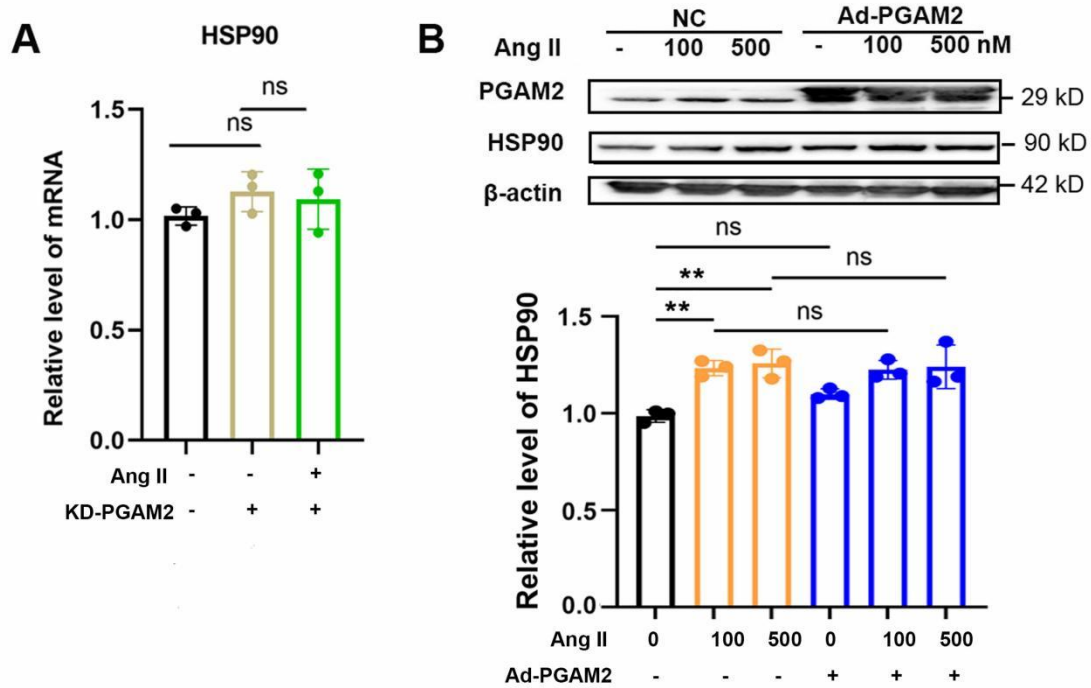
234



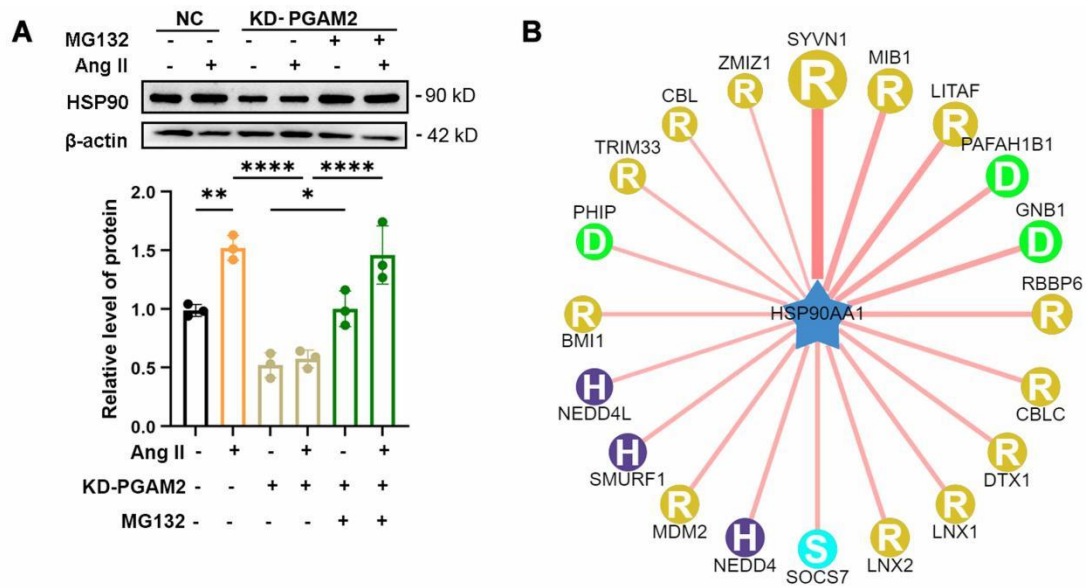
235

236 **Supplementary Figure S5.** The expression of HSP90 and PGAM2 in HSP90

237 knockdown NRVMs followed by Ang II treatment. (A) Representative western  
 238 blotting for HSP90 and PGAM2 under different stimulation and (B-C) densitometric  
 239 quantification (\*,  $P < 0.05$ . \*\*\*,  $P < 0.001$ . \*\*\*\*,  $P < 0.0001$ . ns,  $P > 0.05$ . n = 3).  
 240

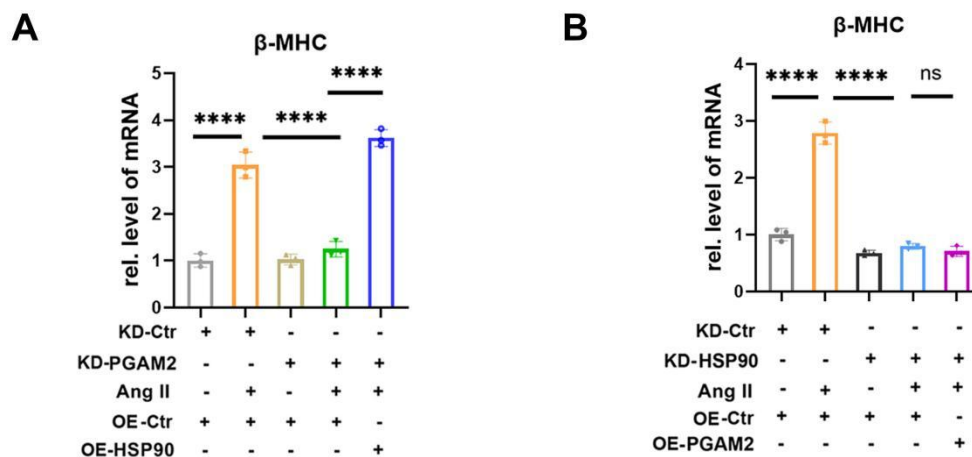


241  
 242 **Supplementary Figure S6.** HSP90 expression in NRVMs with PGAM2 knockdown  
 243 (KD-PGAM2) or overexpression (Ad-PGAM2). (A) qPCR analysis of the mRNA  
 244 levels of HSP90 in NRVMs with KD-PGAM2 followed by Ang II stimulation. (B)  
 245 Representative western blotting for HSP90 and PGAM2 in Ad-PGAM2 NRVMs and  
 246 densitometric quantification for HSP90 (\*\*,  $P < 0.01$ . ns,  $P > 0.05$ . n = 3).  
 247



248

249 **Supplementary Figure S7.** The effects of MG132 on the expression of HSP90 under  
 250 various treatments. (A) Representative western blotting for HSP90 and densitometric  
 251 quantification (\*,  $P < 0.05$ . \*\*,  $P < 0.01$ . \*\*\*\*,  $P < 0.0001$ .  $n = 3$ ). (B) Prediction of  
 252 the E3 ubiquitin ligase of HSP90 through online prediction tool ubibrowser  
 253 (<http://ubibrowser.ncpsb.org/ubibrowser/>).

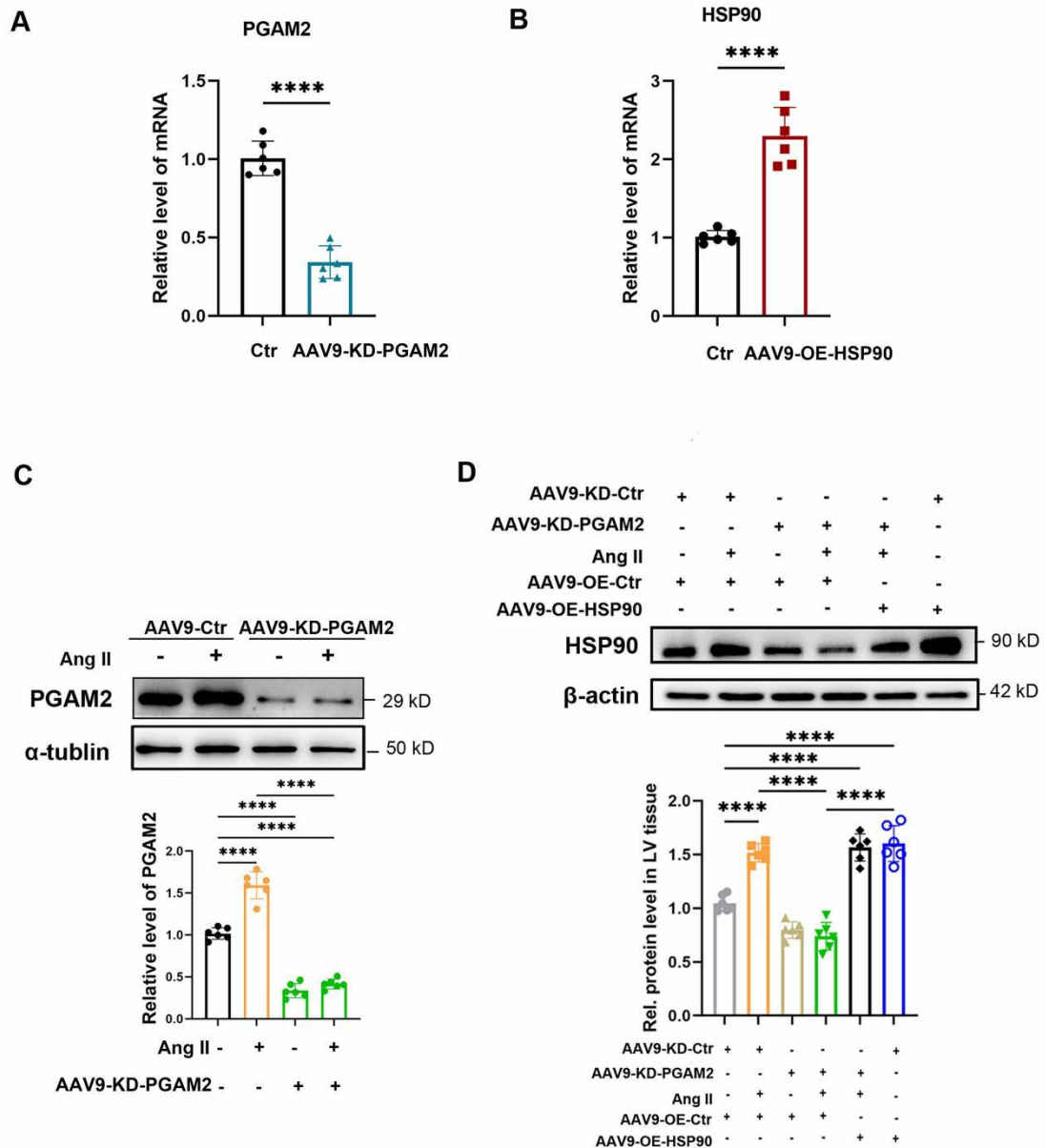


254

255 **Supplementary Figure S8.** The mRNA levels of  $\beta$ -MHC after different treatment. (A)  
 256 Cardiac hypertrophy indicators  $\beta$ -MHC levels were determined by qPCR in NRVMs  
 257 with either PGAM2 knockdown or overexpression of HSP90.  $n = 3$ . (B)  $\beta$ -MHC  
 258 levels were detected after HSP90 knockdown or PGAM2 overexpression using qPCR  
 259 (\*\*\*\*,  $P < 0.0001$ . ns,  $P > 0.05$ .  $n = 3$ ).

260

261



262

263

264

265

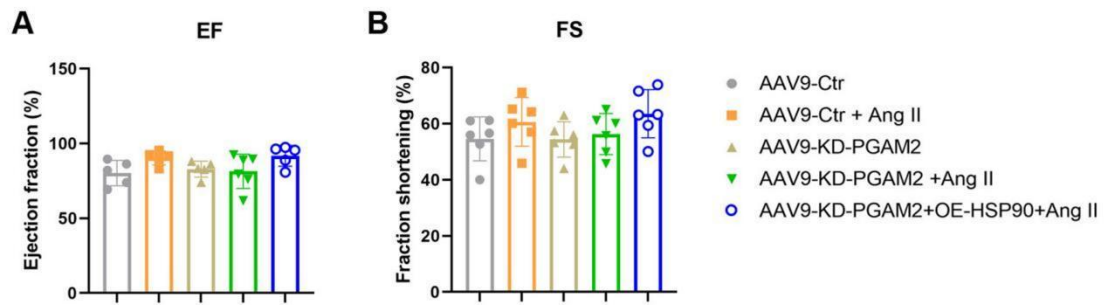
266

267

268

**Supplementary Figure S9.** The efficiency of PGAM2 knockdown and HSP90 overexpression in heart tissue were detected by qPCR and western blotting. (A) RNAi efficiency of PGAM2 detected by qPCR, n = 6; (B) The over-expression efficiency of HSP90 was detected by qPCR, n = 6. Representative western blotting for (C) PGAM2 and (D) HSP90 under various stimulation conditions, n = 6. (\*\*\*\*,  $P < 0.0001$ ).





269

270 **Supplementary Figure S10.** (A) EF and (B) FS were quantified with  
 271 echocardiography in different groups.